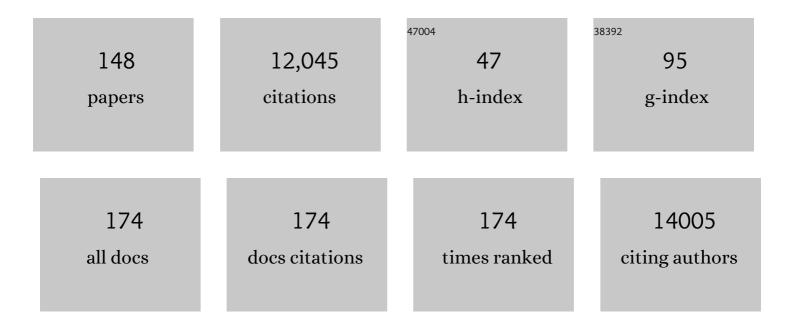
List of Publications by Year in descending order

Source: https://exaly.com/author-pdf/1738247/publications.pdf Version: 2024-02-01



#	Article	IF	CITATIONS
1	Benchmarking of participant-level confound regression strategies for the control of motion artifact in studies of functional connectivity. NeuroImage, 2017, 154, 174-187.	4.2	842
2	Harmonization of cortical thickness measurements across scanners and sites. Neurolmage, 2018, 167, 104-120.	4.2	790
3	Harmonization of multi-site diffusion tensor imaging data. Neurolmage, 2017, 161, 149-170.	4.2	731
4	On testing for spatial correspondence between maps of human brain structure and function. NeuroImage, 2018, 178, 540-551.	4.2	441
5	The extent and drivers of gender imbalance in neuroscience reference lists. Nature Neuroscience, 2020, 23, 918-926.	14.8	327
6	Linked dimensions of psychopathology and connectivity in functional brain networks. Nature Communications, 2018, 9, 3003.	12.8	323
7	Modular Segregation of Structural Brain Networks Supports the Development of Executive Function in Youth. Current Biology, 2017, 27, 1561-1572.e8.	3.9	305
8	Statistical normalization techniques for magnetic resonance imaging. NeuroImage: Clinical, 2014, 6, 9-19.	2.7	300
9	Development of structure–function coupling in human brain networks during youth. Proceedings of the National Academy of Sciences of the United States of America, 2020, 117, 771-778.	7.1	296
10	Statistical harmonization corrects site effects in functional connectivity measurements from multiâ€site fMRI data. Human Brain Mapping, 2018, 39, 4213-4227.	3.6	295
11	Quantitative assessment of structural image quality. NeuroImage, 2018, 169, 407-418.	4.2	291
12	SpaGCN: Integrating gene expression, spatial location and histology to identify spatial domains and spatially variable genes by graph convolutional network. Nature Methods, 2021, 18, 1342-1351.	19.0	291
13	The central vein sign and its clinical evaluation for the diagnosis of multiple sclerosis: a consensus statement from the North American Imaging in Multiple Sclerosis Cooperative. Nature Reviews Neurology, 2016, 12, 714-722.	10.1	274
14	Harmonization of large MRI datasets for the analysis of brain imaging patterns throughout the lifespan. NeuroImage, 2020, 208, 116450.	4.2	260
15	Large-scale Radiomic Profiling of Recurrent Glioblastoma Identifies an Imaging Predictor for Stratifying Anti-Angiogenic Treatment Response. Clinical Cancer Research, 2016, 22, 5765-5771.	7.0	230
16	Normative brain size variation and brain shape diversity in humans. Science, 2018, 360, 1222-1227.	12.6	194
17	Common and Dissociable Mechanisms of Executive System Dysfunction Across Psychiatric Disorders in Youth. American Journal of Psychiatry, 2016, 173, 517-526.	7.2	191
18	Neurological Injury in Adults Treated With Extracorporeal Membrane Oxygenation. Archives of Neurology, 2011, 68, 1543.	4.5	190

#	Article	IF	CITATIONS
19	Radiomic subtyping improves disease stratification beyond key molecular, clinical, and standard imaging characteristics in patients with glioblastoma. Neuro-Oncology, 2018, 20, 848-857.	1.2	170
20	Impact of puberty on the evolution of cerebral perfusion during adolescence. Proceedings of the National Academy of Sciences of the United States of America, 2014, 111, 8643-8648.	7.1	169
21	Individual Variation in Functional Topography of Association Networks in Youth. Neuron, 2020, 106, 340-353.e8.	8.1	162
22	Two distinct neuroanatomical subtypes of schizophrenia revealed using machine learning. Brain, 2020, 143, 1027-1038.	7.6	158
23	Burden of Environmental Adversity Associated With Psychopathology, Maturation, and Brain Behavior Parameters in Youths. JAMA Psychiatry, 2019, 76, 966.	11.0	157
24	Glutamate imaging (GluCEST) lateralizes epileptic foci in nonlesional temporal lobe epilepsy. Science Translational Medicine, 2015, 7, 309ra161.	12.4	156
25	The impact of peppermint oil on the irritable bowel syndrome: a meta-analysis of the pooled clinical data. BMC Complementary and Alternative Medicine, 2019, 19, 21.	3.7	153
26	Childhood trauma history is linked to abnormal brain connectivity in major depression. Proceedings of the National Academy of Sciences of the United States of America, 2019, 116, 8582-8590.	7.1	151
27	Common Dimensional Reward Deficits Across Mood and Psychotic Disorders: A Connectome-Wide Association Study. American Journal of Psychiatry, 2017, 174, 657-666.	7.2	147
28	Increased power by harmonizing structural MRI site differences with the ComBat batch adjustment method in ENIGMA. NeuroImage, 2020, 218, 116956.	4.2	135
29	Longitudinal ComBat: A method for harmonizing longitudinal multi-scanner imaging data. NeuroImage, 2020, 220, 117129.	4.2	132
30	Structural Brain Abnormalities in Youth With Psychosis Spectrum Symptoms. JAMA Psychiatry, 2016, 73, 515.	11.0	116
31	Cancer imaging phenomics toolkit: quantitative imaging analytics for precision diagnostics and predictive modeling of clinical outcome. Journal of Medical Imaging, 2018, 5, 1.	1.5	110
32	Removing inter-subject technical variability in magnetic resonance imaging studies. NeuroImage, 2016, 132, 198-212.	4.2	107
33	Topologically Dissociable Patterns of Development of the Human Cerebral Cortex. Journal of Neuroscience, 2015, 35, 599-609.	3.6	103
34	Volumetric Analysis from a Harmonized Multisite Brain MRI Study of a Single Subject with Multiple Sclerosis. American Journal of Neuroradiology, 2017, 38, 1501-1509.	2.4	95
35	Evaluating White Matter Lesion Segmentations with Refined SÃ,rensen-Dice Analysis. Scientific Reports, 2020, 10, 8242.	3.3	94
36	Virtual resection predicts surgical outcome for drug-resistant epilepsy. Brain, 2019, 142, 3892-3905.	7.6	93

RUSSELL T SHINOHARA

#	Article	IF	CITATIONS
37	Tracheobronchomalacia Is Associated with Increased Morbidity in Bronchopulmonary Dysplasia. Annals of the American Thoracic Society, 2017, 14, 1428-1435.	3.2	90
38	Temporal sequences of brain activity at rest are constrained by white matter structure and modulated by cognitive demands. Communications Biology, 2020, 3, 261.	4.4	88
39	Elevated Amygdala Perfusion Mediates Developmental Sex Differences in Trait Anxiety. Biological Psychiatry, 2016, 80, 775-785.	1.3	82
40	OASIS is Automated Statistical Inference for Segmentation, with applications to multiple sclerosis lesion segmentation in MRI. NeuroImage: Clinical, 2013, 2, 402-413.	2.7	80
41	Cognitive behavioral therapy increases amygdala connectivity with the cognitive control network in both MDD and PTSD. Neurolmage: Clinical, 2017, 14, 464-470.	2.7	78
42	Evidence for Dissociable Linkage of Dimensions of Psychopathology to Brain Structure in Youths. American Journal of Psychiatry, 2019, 176, 1000-1009.	7.2	77
43	Leveraging multi-shell diffusion for studies of brain development in youth and young adulthood. Developmental Cognitive Neuroscience, 2020, 43, 100788.	4.0	65
44	Mapping the structural and functional network architecture of the medial temporal lobe using 7T MRI. Human Brain Mapping, 2018, 39, 851-865.	3.6	60
45	Spatial distribution of interictal spikes fluctuates over time and localizes seizure onset. Brain, 2020, 143, 554-569.	7.6	60
46	Longitudinal Development of Brain Iron Is Linked to Cognition in Youth. Journal of Neuroscience, 2020, 40, 1810-1818.	3.6	60
47	Diastolic Dysfunction Increases the Risk of Primary Graft Dysfunction after Lung Transplant. American Journal of Respiratory and Critical Care Medicine, 2016, 193, 1392-1400.	5.6	58
48	Interpreting support vector machine models for multivariate group wise analysis in neuroimaging. Medical Image Analysis, 2015, 24, 190-204.	11.6	57
49	Predictors of Catastrophic AdverseÂOutcomes in Children With Pulmonary Hypertension Undergoing Cardiac Catheterization. Journal of the American College of Cardiology, 2015, 66, 1261-1269.	2.8	57
50	Characterizing the role of the structural connectome in seizure dynamics. Brain, 2019, 142, 1955-1972.	7.6	56
51	Diminished Cortical Thickness Is Associated with Impulsive Choice in Adolescence. Journal of Neuroscience, 2018, 38, 2471-2481.	3.6	55
52	The Challenges with Brain Death Determination in Adult Patients on Extracorporeal Membrane Oxygenation. Neurocritical Care, 2011, 14, 423-426.	2.4	53
53	Imaging outcome measures of neuroprotection and repair in MS. Neurology, 2019, 92, 519-533.	1.1	53
54	Glutamate weighted imaging contrast in gliomas with 7†Tesla magnetic resonance imaging. NeuroImage: Clinical, 2019, 22, 101694.	2.7	50

RUSSELL T SHINOHARA

#	Article	IF	CITATIONS
55	Pitfalls in brain age analyses. Human Brain Mapping, 2021, 42, 4092-4101.	3.6	50
56	Structural and functional asymmetry of medial temporal subregions in unilateral temporal lobe epilepsy: A 7T MRI study. Human Brain Mapping, 2019, 40, 2390-2398.	3.6	49
57	Mitigating site effects in covariance for machine learning in neuroimaging data. Human Brain Mapping, 2022, 43, 1179-1195.	3.6	49
58	Worldwide Reported Use of IV Tissue Plasminogen Activator for Acute Ischemic Stroke. International Journal of Stroke, 2014, 9, 349-355.	5.9	47
59	Optimization of energy state transition trajectory supports the development of executive function during youth. ELife, 2020, 9, .	6.0	47
60	MIMoSA: An Automated Method for Intermodal Segmentation Analysis of Multiple Sclerosis Brain Lesions. Journal of Neuroimaging, 2018, 28, 389-398.	2.0	44
61	Structural Correlationâ€based Outlier Rejection (SCORE) algorithm for arterial spin labeling time series. Journal of Magnetic Resonance Imaging, 2017, 45, 1786-1797.	3.4	42
62	A surfaceâ€in gradient of thalamic damage evolves in pediatric multiple sclerosis. Annals of Neurology, 2019, 85, 340-351.	5.3	42
63	Population-wide principal component-based quantification of blood–brain-barrier dynamics in multiple sclerosis. NeuroImage, 2011, 57, 1430-1446.	4.2	40
64	Addressing Confounding in Predictive Models with an Application to Neuroimaging. International Journal of Biostatistics, 2016, 12, 31-44.	0.7	39
65	Resting fMRI-guided TMS results in subcortical and brain network modulation indexed by interleaved TMS/fMRI. Experimental Brain Research, 2021, 239, 1165-1178.	1.5	39
66	A Comparison of Supervised Machine Learning Algorithms and Feature Vectors for MS Lesion Segmentation Using Multimodal Structural MRI. PLoS ONE, 2014, 9, e95753.	2.5	38
67	Power estimation for non-standardized multisite studies. NeuroImage, 2016, 134, 281-294.	4.2	36
68	Cost comparison of Transcatheter and Operative Pulmonary Valve Replacement (from the Pediatric) Tj ETQqO (	) 0 rgBT /O	verlock 10 Tf 5
69	Effect of center catheterization volume on risk of catastrophic adverse event after cardiac catheterization in children. American Heart Journal, 2015, 169, 823-832.e5.	2.7	35
70	Neurostructural Heterogeneity in Youths With Internalizing Symptoms. Biological Psychiatry, 2020, 87, 473-482.	1.3	34
71	Sex Differences in Variability of Brain Structure Across the Lifespan. Cerebral Cortex, 2020, 30, 5420-5430.	2.9	33
72	Network changes associated with transdiagnostic depressive symptom improvement following cognitive behavioral therapy in MDD and PTSD. Molecular Psychiatry, 2018, 23, 2314-2323.	7.9	30

#	Article	IF	CITATIONS
73	Approaches to Defining Common and Dissociable Neurobiological Deficits Associated With Psychopathology in Youth. Biological Psychiatry, 2020, 88, 51-62.	1.3	30
74	Automated Integration of Multimodal MRI for the Probabilistic Detection of the Central Vein Sign in White Matter Lesions. American Journal of Neuroradiology, 2018, 39, 1806-1813.	2.4	29
75	Normative intracranial EEG maps epileptogenic tissues in focal epilepsy. Brain, 2022, 145, 1949-1961.	7.6	29
76	Cost comparison of transcatheter and operative closures of ostium secundum atrial septal defects. American Heart Journal, 2015, 169, 727-735.e2.	2.7	28
77	Sex-biased trajectories of amygdalo-hippocampal morphology change over human development. NeuroImage, 2020, 204, 116122.	4.2	28
78	Vitamin D levels do not predict the stage of hepatic fibrosis in patients with non-alcoholic fatty liver disease: A PRISMA compliant systematic review and meta-analysis of pooled data. World Journal of Hepatology, 2018, 10, 142-154.	2.0	28
79	Multi-scale semi-supervised clustering of brain images: Deriving disease subtypes. Medical Image Analysis, 2022, 75, 102304.	11.6	28
80	Gradient nonlinearity effects on upper cervical spinal cord area measurement from 3D T <sub>1</sub> â€weighted brain MRI acquisitions. Magnetic Resonance in Medicine, 2018, 79, 1595-1601.	3.0	27
81	Neuroimaging Findings in US Government Personnel With Possible Exposure to Directional Phenomena in Havana, Cuba. JAMA - Journal of the American Medical Association, 2019, 322, 336.	7.4	27
82	Multisite reliability and repeatability of an advanced brain MRI protocol. Journal of Magnetic Resonance Imaging, 2019, 50, 878-888.	3.4	27
83	Comparative effectiveness of less commonly used systemic monotherapies and common combination therapies for moderate to severe psoriasis in the clinical setting. Journal of the American Academy of Dermatology, 2014, 71, 1167-1175.	1.2	26
84	Accelerated cortical thinning within structural brain networks is associated with irritability in youth. Neuropsychopharmacology, 2019, 44, 2254-2262.	5.4	26
85	Singleâ€Voxel <sup>1</sup> H MR spectroscopy of cerebral nicotinamide adenine dinucleotide (NAD <sup>+</sup> ) in humans at 7T using a 32â€channel volume coil. Magnetic Resonance in Medicine, 2020, 83, 806-814.	3.0	26
86	Overall survival prediction in glioblastoma patients using structural magnetic resonance imaging (MRI): advanced radiomic features may compensate for lack of advanced MRI modalities. Journal of Medical Imaging, 2020, 7, 1.	1.5	26
87	Reproducibility analysis of multiâ€institutional paired expert annotations and radiomic features of the Ivy Clioblastoma Atlas Project (Ivy GAP) dataset. Medical Physics, 2020, 47, 6039-6052.	3.0	25
88	Generalized ComBat harmonization methods for radiomic features with multi-modal distributions and multiple batch effects. Scientific Reports, 2022, 12, 4493.	3.3	25
89	An Automated Statistical Technique for Counting Distinct Multiple Sclerosis Lesions. American Journal of Neuroradiology, 2018, 39, 626-633.	2.4	24
90	Imaging Mechanisms of Disease Progression in Multiple Sclerosis: Beyond Brain Atrophy. Journal of Neuroimaging, 2020, 30, 251-266.	2.0	24

#	Article	IF	CITATIONS
91	Multiâ€scale network regression for brainâ€phenotype associations. Human Brain Mapping, 2020, 41, 2553-2566.	3.6	24
92	Imaging local genetic influences on cortical folding. Proceedings of the National Academy of Sciences of the United States of America, 2020, 117, 7430-7436.	7.1	24
93	Structural and Functional Brain Parameters Related to Cognitive Performance Across Development: Replication and Extension of the Parieto-Frontal Integration Theory in a Single Sample. Cerebral Cortex, 2021, 31, 1444-1463.	2.9	24
94	Influence of vitamin D on liver fibrosis in chronic hepatitis C: A systematic review and meta-analysis of the pooled clinical trials data. World Journal of Hepatology, 2017, 9, 278.	2.0	24
95	Subject-level measurement of local cortical coupling. NeuroImage, 2016, 133, 88-97.	4.2	23
96	Control-group feature normalization for multivariate pattern analysis of structural MRI data using the support vector machine. Neurolmage, 2016, 132, 157-166.	4.2	23
97	Developmental coupling of cerebral blood flow and fMRI fluctuations in youth. Cell Reports, 2022, 38, 110576.	6.4	23
98	Structural brain measures linked to clinical phenotypes in major depression replicate across clinical centres. Molecular Psychiatry, 2021, 26, 2764-2775.	7.9	21
99	A framework For brain atlases: Lessons from seizure dynamics. Neurolmage, 2022, 254, 118986.	4.2	20
100	Clinical measures, radiomics, and genomics offer synergistic value in AI-based prediction of overall survival in patients with glioblastoma. Scientific Reports, 2022, 12, .	3.3	20
101	Health Effects of Lesion Localization in Multiple Sclerosis: Spatial Registration and Confounding Adjustment. PLoS ONE, 2014, 9, e107263.	2.5	19
102	Harmonizing functional connectivity reduces scanner effects in community detection. Neurolmage, 2022, 256, 119198.	4.2	19
103	Relating multi-sequence longitudinal intensity profiles and clinical covariates in incident multiple sclerosis lesions. NeuroImage: Clinical, 2016, 10, 1-17.	2.7	18
104	White matter microstructural deficits in 22q11.2 deletion syndrome. Psychiatry Research - Neuroimaging, 2017, 268, 35-44.	1.8	17
105	Statistical estimation of T1 relaxation times using conventional magnetic resonance imaging. NeuroImage, 2016, 133, 176-188.	4.2	16
106	A dual modeling approach to automatic segmentation of cerebral T2 hyperintensities and T1 black holes in multiple sclerosis. NeuroImage: Clinical, 2018, 20, 1211-1221.	2.7	16
107	A simple permutationâ€based test of intermodal correspondence. Human Brain Mapping, 2021, 42, 5175-5187.	3.6	16
108	A Multicenter Cohort Study of Inferior Vena Cava Filter Use in Children. Pediatric Blood and Cancer, 2015, 62, 2089-2093.	1.5	15

#	Article	IF	CITATIONS
109	Stroke in HIV-infected African Americans: a retrospective cohort study. Journal of NeuroVirology, 2016, 22, 50-55.	2.1	15
110	Recovery kinetics of creatine in mild plantar flexion exercise using 3D creatine CEST imaging at 7 Tesla. Magnetic Resonance in Medicine, 2021, 85, 802-817.	3.0	15
111	Statistical estimation of white matter microstructure from conventional MRI. NeuroImage: Clinical, 2016, 12, 615-623.	2.7	12
112	The NAIMS cooperative pilot project: Design, implementation and future directions. Multiple Sclerosis Journal, 2018, 24, 1770-1772.	3.0	12
113	The emergent integrated network structure of scientific research. PLoS ONE, 2019, 14, e0216146.	2.5	12
114	Multiple sclerosis diagnosis: Knowledge gaps and opportunities for educational intervention in neurologists in the United States. Multiple Sclerosis Journal, 2022, 28, 1248-1256.	3.0	12
115	Multi-institutional noninvasive in vivo characterization of <i>IDH</i> , 1p/19q, and EGFRvIII in glioma using neuro-Cancer Imaging Phenomics Toolkit (neuro-CaPTk). Neuro-Oncology Advances, 2020, 2, iv22-iv34.	0.7	12
116	Privacy-preserving harmonization via distributed ComBat. NeuroImage, 2022, 248, 118822.	4.2	11
117	Diminished reward responsiveness is associated with lower reward network GluCEST: an ultra-high field glutamate imaging study. Molecular Psychiatry, 2021, 26, 2137-2147.	7.9	10
118	Fully automated detection of paramagnetic rims in multiple sclerosis lesions on 3T susceptibility-based MR imaging. NeuroImage: Clinical, 2021, 32, 102796.	2.7	10
119	Accuracy of Transthoracic Echocardiography in Assessing Retro-aortic Rim prior to Device Closure of Atrial Septal Defects. Congenital Heart Disease, 2015, 10, E146-E154.	0.2	9
120	The landscape of NeuroImage-ing research. NeuroImage, 2018, 183, 872-883.	4.2	9
121	Multidimensional brain-age prediction reveals altered brain developmental trajectory in psychiatric disorders. Cerebral Cortex, 2022, 32, 5036-5049.	2.9	9
122	PREVAIL: Predicting Recovery through Estimation and Visualization of Active and Incident Lesions. NeuroImage: Clinical, 2016, 12, 293-299.	2.7	8
123	Alterations in white matter microstructure in individuals at persistent risk for psychosis. Molecular Psychiatry, 2020, 25, 2441-2454.	7.9	8
124	Dimensional connectomics of anxious misery, a human connectome study related to human disease: Overview of protocol and data quality. NeuroImage: Clinical, 2020, 28, 102489.	2.7	8
125	Robust Spatial Extent Inference With a Semiparametric Bootstrap Joint Inference Procedure. Biometrics, 2019, 75, 1145-1155.	1.4	7
126	TAPAS: A Thresholding Approach for Probability Map Automatic Segmentation in Multiple Sclerosis. NeuroImage: Clinical, 2020, 27, 102256.	2.7	5

#	Article	IF	CITATIONS
127	Dice Overlap Measures for Objects of Unknown Number: Application to Lesion Segmentation. Lecture Notes in Computer Science, 2018, 10670, 3-14.	1.3	5
128	Leveraging machine learning predictive biomarkers to augment the statistical power of clinical trials with baseline magnetic resonance imaging. Brain Communications, 2021, 3, fcab264.	3.3	5
129	Scanâ€stratified caseâ€control sampling for modeling blood–brain barrier integrity in multiple sclerosis. Statistics in Medicine, 2015, 34, 2872-2880.	1.6	4
130	Voxelâ€wise intermodal coupling analysis of two or more modalities using local covariance decomposition. Human Brain Mapping, 2022, 43, 4650-4663.	3.6	4
131	Automated Analysis of Low-Field Brain MRI in Cerebral Malaria. Biometrics, 2023, 79, 2417-2429.	1.4	4
132	A Broad Symmetry Criterion for Nonparametric Validity of Parametrically Based Tests in Randomized Trials. Biometrics, 2012, 68, 85-91.	1.4	3
133	Estimating parsimonious models of longitudinal causal effects using regressions on propensity scores. Statistics in Medicine, 2013, 32, 3829-3837.	1.6	3
134	A Pilot Trial to Examine the Effect of High-Dose Niacin on Arterial Wall Inflammation Using Fluorodeoxyglucose Positron Emission Tomography. Academic Radiology, 2015, 22, 600-609.	2.5	3
135	Alternating event processes during lifetimes: population dynamics and statistical inference. Lifetime Data Analysis, 2018, 24, 110-125.	0.9	3
136	Experimental design and sample size considerations in longitudinal magnetic resonance imaging-based biomarker detection for multiple sclerosis. Statistical Methods in Medical Research, 2020, 29, 2617-2628.	1.5	3
137	Nonnegative decomposition of functional count data. Biometrics, 2020, 76, 1273-1284.	1.4	3
138	Connectome-wide Functional Connectivity Abnormalities in Youth With Obsessive-Compulsive Symptoms. Biological Psychiatry: Cognitive Neuroscience and Neuroimaging, 2022, 7, 1068-1077.	1.5	3
139	Statistical approaches to temporal and spatial autocorrelation in resting-state functional connectivity in mice measured with optical intrinsic signal imaging. Neurophotonics, 2022, 9, 041405.	3.3	3
140	Soft Null Hypotheses: A Case Study of Image Enhancement Detection in Brain Lesions. Journal of Computational and Graphical Statistics, 2016, 25, 570-588.	1.7	2
141	Interpretable High-Dimensional Inference Via Score Projection With an Application in Neuroimaging. Journal of the American Statistical Association, 2019, 114, 820-830.	3.1	2
142	Distanceâ€based analysis of variance for brain connectivity. Biometrics, 2020, 76, 257-269.	1.4	2
143	Joint Intensity Fusion Image Synthesis Applied to Multiple Sclerosis Lesion Segmentation. , 2018, 10670, 43-54.		2
144	Multisite MRI reproducibility of lateral ventricular volume using the NAIMS cooperative pilot dataset. Journal of Neuroimaging, 2022, 32, 910-919.	2.0	2

#	Article	IF	CITATIONS
145	A local group differences test for subject-level multivariate density neuroimaging outcomes. Biostatistics, 2021, 22, 646-661.	1.5	1
146	Matrix decomposition for modeling lesion development processes in multiple sclerosis. Biostatistics, 2022, 23, 83-100.	1.5	1
147	Multiple Sclerosis Lesion Segmentation Using Joint Label Fusion. Lecture Notes in Computer Science, 2017, 10530, 138-145.	1.3	1
148	Bayesian Spatial Binary Regression for Label Fusion in Structural Neuroimaging. Journal of the American Statistical Association, 0, , 1-14.	3.1	0